

## EXPERIMENTAL STUDY ON HEAT TRANSFER CHARACTERISTICS OF DIMPLED SURFACE THERMOSYPHON WITH $Al_2O_3$ NANOFLUID

by

**Siva Subramanian RAJESWARAN<sup>a</sup>, Kumaresan GOVINDASAMY<sup>b\*</sup>,  
Selvakumar PANDIARAJ<sup>c</sup>, and Kamatchi RAJARAM<sup>d</sup>**

<sup>a</sup>Department of Mechanical Engineering, Sri Krishna College of Engineering and Technology, Coimbatore, Tamil Nadu, India

<sup>b</sup>Department of Mechanical Engineering, Bannari Amman Institute of Technology, Sathyamangalam, Tamil Nadu, India

<sup>c</sup>Department of Mechanical Engineering, Kongu Engineering College, Erode, Tamil Nadu, India

<sup>d</sup>School of Mechanical Engineering, VIT University, Vellore, Tamil Nadu, India

Original scientific paper

<https://doi.org/10.2298/TSCI230816267R>

*The current research on boiling in heat transfer applications has been increased due to the effective heat dissipation rate in solar applications, cooling of new generation electronic chips with the goal of improving performance by controlling physical factors. Thermosyphons are one among the phase change medium which has the higher critical heat flux to accelerate the heat transfer. Current work in Thermosyphon focuses on the design, fabrication, and performance analysis of dimpled thermosyphon with certain variables like surface area of heat exchange, composition of working fluid and setup angle. Due to the impact of nanotechnology, the investigation is carried out by using  $Al_2O_3$  nanofluid as working fluid. The experiments are conducted initially with plain thermosyphons, later with surface modifications (dimple) by changing the orientation of the thermosyphons. The performance results of the plain thermosyphon filled with water, plain thermosyphon filled with nanofluid is compared with dimpled thermosyphon with nanofluid at different angles such as  $0^\circ$ ,  $45^\circ$ , and  $90^\circ$ . Evaporator side dimple and condenser side dimple also designed and investigated. It is observed that thermal resistance for dimple thermosyphon-nanofluid is very low in the range of  $0.06$ - $0.20$   $^\circ C/W$  when compared with plain thermosyphon-water varies from  $0.1$ - $0.45$   $^\circ C/W$ , for plain thermosyphon-nanofluid is  $0.1$ - $0.31$   $^\circ C/W$ . It is also observed that the efficiency of dimpled tube Thermosyphon with Nanofluid is estimated as  $50.66\%$ ,  $69.7\%$ , and  $74.23\%$  at  $0^\circ$ ,  $45^\circ$ , and  $90^\circ$ , respectively, which is the maximum value when compared with plain thermosyphon with water and nanofluid.*

Key words: *dimpled thermosyphon,  $Al_2O_3$  nanofluid, characterization, performance*

### Introduction

In recent days, the combination of nanoscience and heat transfer researches are engraving their footprints on the major applications such as cooling of electronic systems, electric

---

\*Corresponding author, e-mail: kumareshgct@gmail.com

vehicle systems, solar applications and semiconductor areas. In cooling of thermal systems, thermosyphon is the major device which connects both research areas. A thermosyphon is one of the passive type cooling system with hot and cold interface ends where the prepared working fluids will take the phase change. At the evaporator side hot interface end, a liquid which is in contact with the hot surface turns into vapor by receiving the heat from the wall surface. This vapor formed travels axially to the cold interface and condenses, where the latent heat is released. Then, condensate will return to the hot end by capillary action, centrifugal force or gravity and the cycle repeats. The thermal conductivity,  $k$ , of the copper Thermosyphon is almost 90 times higher than that of a normal bar made of copper with the same configuration [1]. Several studies concluded that the thermosyphons are good choice for the thermal management of all computer accessories [2-4], electronic circuits cooling [5-7], battery cooling of electric vehicles [8-11], and solar applications [12, 13]. So, the current study has been chosen. The thermosyphons with different geometry due to higher demand in better cooling, need of the larger ability in transferring heat in low thermal gradient and low weight applications. The wick structure's capillary pressure limits the heat transport characteristics of applications at moderate temperatures [14]. The wick material's porosity and permeability, as well as the mass-flow rate of the working fluid that is utilized, all have an impact on the evaporator's heat resistance [15]. For the purpose of improving heat transfer process, the evaporation properties of various wick micro-structures were the subject of experimental research [16]. The experiments were conducted on different geometrics such as flat heat pipes without fins [17], with array of fins, with internal grooved heat pipes, mesh type of internal wicked heat pipes [18], sintered metal evil intensity heat pipes [19], and ultra-thin flat heat pipes [20] were previously reported. In recent researches, liquids with nanoparticles (more modest than 100 nm) have an extraordinary potential in heat transfer enhancement using the heat pipes. Inclusion of nanoparticles in fluids will drastically alter the thermophysical properties conventional fluids [21]. A study reported that, the performance of two phase closed thermosyphon with aqueous  $\text{Al}_2\text{O}_3$  nanoparticles of volume concentration of 1-3%. The experimental results indicated that the two phase closed thermosyphon efficiency increased by up to 14.7% for various input powers [19]. In a similar vein, the effectiveness of various nanofluids in a heat pipe evacuated tube solar collector was the subject of numerous experimental studies. A review noticed the issue of settling down of nanoparticles with a somewhat huge load of  $\text{Al}_2\text{O}_3$  nanofluid. At the same testing conditions, the nanofluids performed better than acetone. It was higher at a volumetric concentration of 0.5%, which was higher than the 0.25% concentration [22]. A similar experiment with  $\text{WO}_3$ -water nanofluid at three different volume fractions of  $\text{WO}_3$  nanoparticles (0.014%, 0.028%, and 0.042%) were examined at several mass-flow rates per unit area are alike 13 g/s per  $\text{m}^2$ , 15 g/s per  $\text{m}^2$ , and 17 g/s per  $\text{m}^2$ . The efficiency of this evacuated tube solar collector is about 72.8%, which is 19.3% higher than water. This complete literature on thermosyphons indicates the usage of thermosyphons in different applications with different geometrics and fluid medium. It is well understood that, the usage of dimpled surface Thermosyphon is very limited and not provided results in various aspects. Hence, the present work identified a new geometric thermosyphon called dimpled surface for any kind of thermosyphon applications. Especially, this work believes that, the dimpled surface thermosyphon may be a right choice for the solar thermal collectors due to high heat transport characteristics. Also in electronic systems and super-computers developed by companies like IBM heat generation is as much as 300 W to 800 W. In such scenarios, thermosyphons are preferred solution due to their compact design and impressive thermal conductivity.

## Thermosyphon and nanofluid preparation methods

### *Characterization of nanoparticles*

The  $\text{Al}_2\text{O}_3$  nanoparticles are produced using sol gel method. Initially, 18.76 g of aluminum nitrate was taken by measuring in a digital weighing scale. It has been dissolved with citric acid in the distilled water. The solution was well stirred at 60 °C, for certain period of time until it becomes yellowish meta-stable solution. Further, the solution was maintained at 80 °C temperature with constant stirring which turns into the transparent gel after some time. The transparent gel was gradually dried at 100 °C in an oven for 12 hours. The dried gel was taken out and sintered at 600 °C to prepare  $\text{Al}_2\text{O}_3$  nanoparticles and considered for characterization process. The phases of the prepared nanoparticles are examined using the XRD model Shimadzu XRD-6000 at room temperature and SEM image was taken at 2000× and 4000× magnification range. The micrograph showed the irregular shape and sponge like structure of nanoparticles.

### *Nanofluid preparation and characterization*

The present work has thought about the spherical  $\text{Al}_2\text{O}_3$  as nanoparticles (50 nm, acceptable diameter, mass per unit volume 3.88 g/cc) and deionized water as the base liquid to set up the nanofluid. Catalytic chemical vapor deposition was used to make  $\text{Al}_2\text{O}_3$  nanoparticles. The number of nanoparticles required to produce a solution with a volume concentration of 3% is calculated. The nanoparticles were dispersed in deionized water using an ultrasonic homogenizer, and the solution was vibrated for 90 minutes to create a uniformly dispersed mixture as shown in fig. 1. Every one of the finished samples must be statically put for 45 days and it is seen that even after 45 days the fluid was stable and did not have much suspension. Thermal conductivity is determined by using KD2 Pro thermal properties analyzer and was 0.625 W/mK and dynamic viscosity is found by using Brook field digital viscometer and was around 1.05 centipoise. Surface Tension was 1.05 MN/m which was found using SITA Tension meter.



Figure 1. Preparation and stability testing of  $\text{Al}_2\text{O}_3$ -deionized water nanofluid

### *Design and fabrication of thermosyphon*

Copper was selected as the material for the thermosyphon because of its higher thermal conductivity and compatibility with selected working medium. In this study, the thermosyphon has a total length of 380 mm, length of the condenser section is 180 mm, length of the evaporator section is 120 mm, an outer diameter of 19 mm, and a thickness of 1 mm, dimple projection was created on the surface of the thermosyphon using a die with 3 mm diameter. The process was carried out in a drilling machine with high precision and pressure. The die is fixed

inside the chuck of vertical drilling machine and is allowed to make punch on the surface of thermosyphon. A uniform pressure is maintained to create uniform dimple formation. Dimple diameter is 3 mm, centre to centre distance between dimples is 12 mm. Nanofluids and deionized water are filled in the thermosyphon. To extract more heat from the thermosyphon than air cooling, the condenser section is cooled by liquid water while the evaporator side is enclosed by a surface electric heater. A variable angle holder is used to adjust the thermosyphon's inclination angle from its horizontal axis to  $0^\circ$ ,  $45^\circ$ , and  $90^\circ$ .

### The 3-D model of the thermosyphon

The design of thermosyphon is carried by using solid works software in three stages like, plain thermosyphon, thermosyphon with dimple on evaporator, and thermosyphon with dimple on condenser. Figures 2(a) and 2(b) shows the 3-D model of thermosyphon with dimple, where the condenser length is assumed higher than evaporator section.

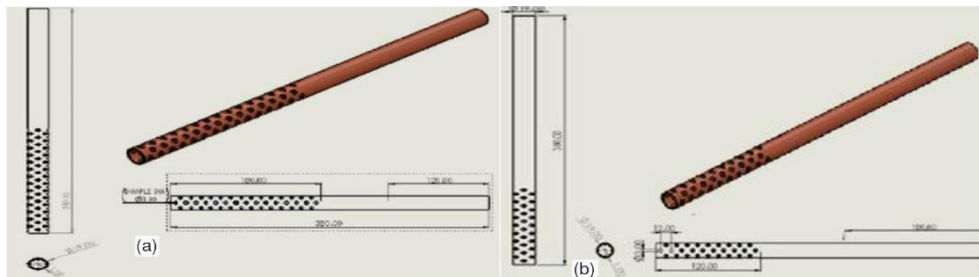


Figure 2. (a) Dimpled condenser surface and (b) dimpled evaporator surface

Figure 3(a) shows that, how the protrusion developed inside the thermosyphon due to the external dimpling. Figure 3(b) shows the analysis of dimple size. The dimple formation has followed the zigzag pattern. From the figure it is understood that, a uniform transverse pitch of 12 mm is maintained. Each dimple is created with 3 mm diameter and 1.5 mm depth approximately.

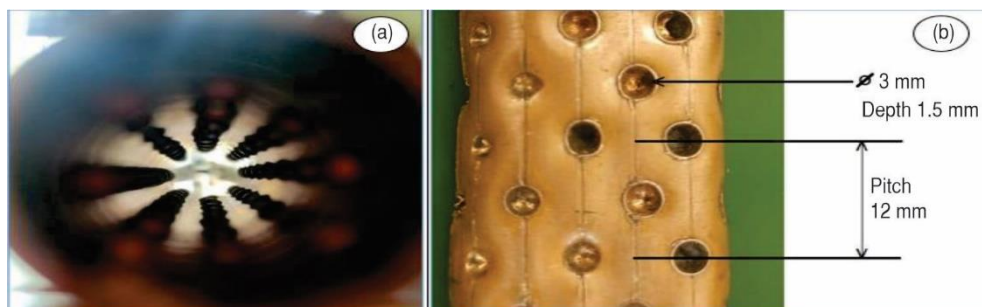


Figure 3. (a) Protrusion inside the pipe and (b) prediction of dimple size

### Experimental set-up

The current experimental apparatus is depicted in fig. 4(a). A preferred test section, a cooling water circuit, and a data acquisition system make up the test circuit. A storage tank with volume of  $0.125 \text{ m}^3$  serves as the source of supply for cold water. A temperature controller controls the flow of cold water before it is pumped out of storage tank. A flow meter is used to

set temperature of cooling water at  $20 \pm 5$  °C and keeping an eye on the fixed flow rate. The thermosyphon of study is a long copper material tube with an outer diameter of 19 mm and a length of 380 mm and 1 mm thick. The condenser segment of thermosyphon was embedded upward into the cooling chamber. The coolant moved through the cooling chamber, where it was forced to condense heat from the condenser section into a bath of constant temperature. Figure 4(b) depicts the dimpled tube during the experiment.

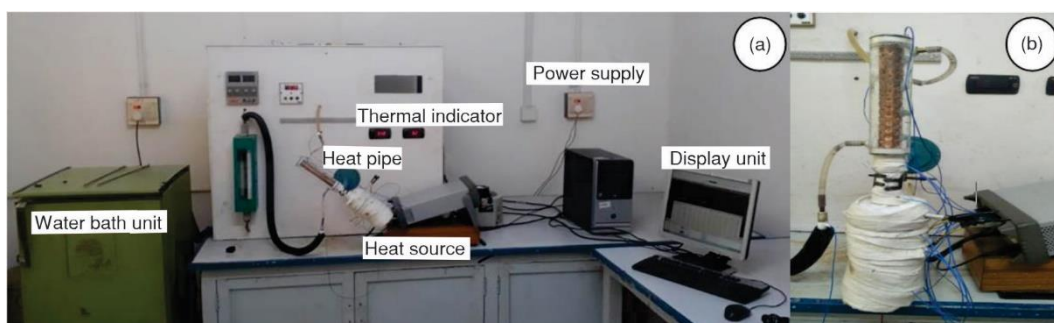


Figure 4. (a) experimental set-up and (b) dimpled thermosyphon during experiment

Figure 5 depicts the schematic layout of thermosyphon with thermocouples located at a distance of 20 mm, 60 mm, 100 mm, 140 mm, 180 mm, 220 mm, 260 mm, 300 mm, and 340 mm from the evaporator end which indicates the measurement of vapor temperature and surface temperature at all locations. The observations are made for plain thermosyphon-water, plain thermosyphon-nanofluid, dimple thermosyphon-nanofluid combinations. In each orientation, four set of trails (eight readings) has been done.

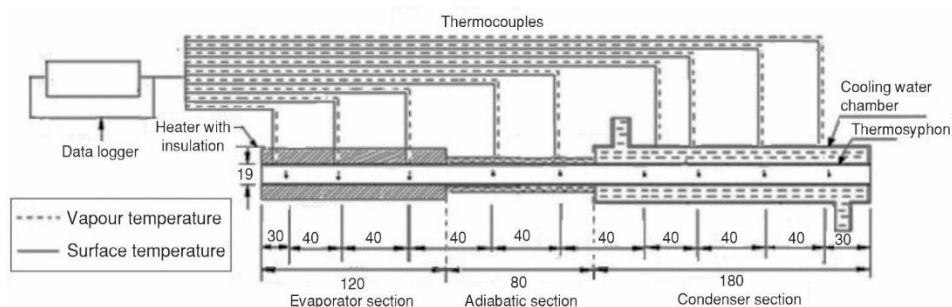


Figure 5. Schematic layout of thermosyphon with thermocouple location

## Results and discussion

The performance of dimpled thermosyphon is influenced by the certain parameters such as evaporator and condenser length, resistance offered by the flow medium, heat supplied and heat transfer rate. These factors are considered for discussion based on the obtained and calculated results.

### *Effect of evaporator length and condenser length*

The evaporator's length is comparatively lesser than the condenser. The investigation is carried out at three orientations such as  $0^\circ$ ,  $45^\circ$ , and  $90^\circ$ . The values obtained at  $90^\circ$  only presented here for discussion. When heat is supplied, the fluid inside the evaporator will absorb

the heat energy from heat source and gets saturated. This flows axially to the adiabatic section, then condenser. Figures 6 and 7 shows the temperature distribution with respect to the distance along flow direction in evaporator and condenser. It is initially showing an incremental temperature distribution measured along the length of condenser and evaporator section in thermosyphons, later it has been reduced gradually for heat inputs 40W, 80W, 120W, 160W, 200W, 240W, and 280 W which clearly infers that there is an increase in heat transfer.

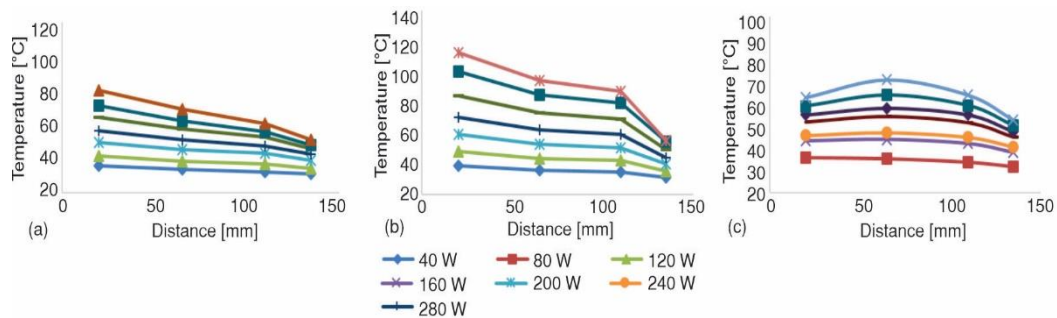


Figure 6. Evaporator temperature; (a) plain pipe-water, (b) plain pipe-nanofluid, and (c) dimple pipe

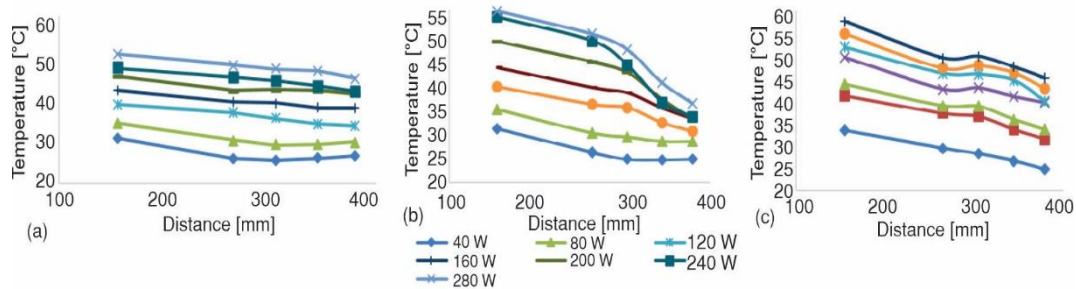


Figure 7. Condenser temperature; (a) plain pipe-water, (b) plain pipe-nanofluid, and (c) dimple pipe

This indicates the tendency of nanofluid to accelerate the heat transfer than normal water. Also, the inside protrusion due to external dimple will interrupt the heat flow and generates the more heat flux which caused the temperature hike up to certain distance, than it reduced towards the condenser as shown in figs. 6 and 7. Similar results have been obtained for 0° and 45° tilt angle. At all inclinations at lowest heat loads the local temperature variation is around 5 °C to 7 °C in both condenser and evaporator and for highest heat loads local temperature variation is around 8 °C to 10 °C in both condenser and evaporator side.

#### Effect of heat input on temperature

Figure 8 indicates the variation of temperature for various heat input with respect to the tilt angle. When the orientation has changed, the free flow of heat is being restricted and evaporator needs to generate more vapor mixture to push up the heat flow. It is found that, the amount of heat required for thermosyphon at tilt angle 45° and 90° is high compared with 0°. At these angles, the initial temperatures are high at evaporator as shown in figs. 8(a)-8(c). At 90° tilt angle the heat flux is high which increases the amount of heat transfer than other two orientations of 0° and 45° tilt angle.

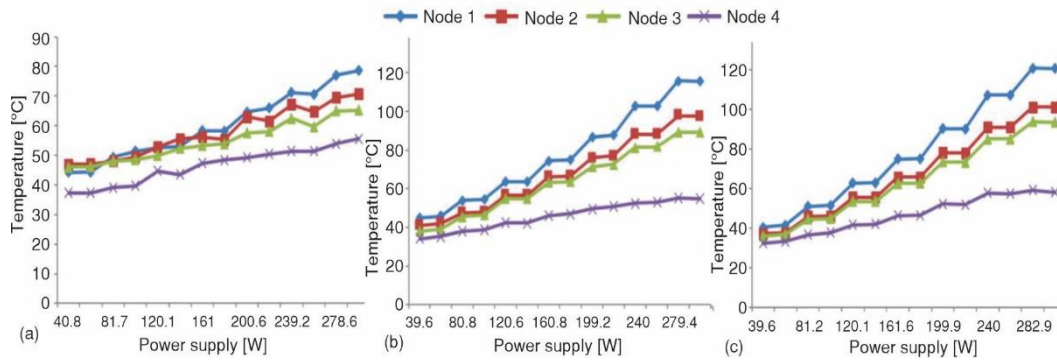


Figure 8. Effect of heat input on temperature distribution; (a) at 0°, (b) at 45°, and (c) at 90°

**Effect of heat input on thermal resistance**

The thermal resistance is a kind of factor which resists the heat flow from the evaporator to the condenser and it influence the heat transfer capacity of the plain or dimpled thermosyphon. It ensures the efficiency of both condenser and the evaporator. This can be estimated by:

$$R = \frac{T_{eva} - T_{con}}{Q_{input}}$$

Figures 9(a)-9(c) shows the thermal resistance value estimated at different angles. From these figures, it is evident that, thermosyphon with dimple surface are showing very less thermal resistance value compared to plain thermosyphon with water and nanofluid which is more important for heat transfer enhancement. As low as the thermal resistance heat transfer will be high as a result of it high rate of vapor formation evaporator occurs. At 90° orientation, dimpled thermosyphon and nanofluid combination has shown better results.

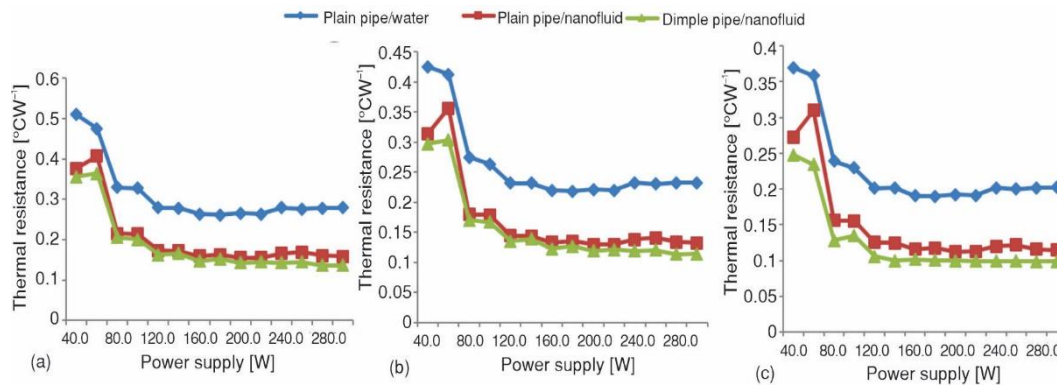


Figure 9. Thermal resistance; (a) at 0°, (b) at 45°, and (c) at 90°

**Effect of heat input on Nusselt number**

The Nusselt number is often used to quantify how effective is the heat transfer enhancement due to convection. From the results obtained the Nusselt number value is calculated

and it is evident that the value of Nusselt number values of dimpled tube thermosyphon at 90° inclination with 3% concentration of Al<sub>2</sub>O<sub>3</sub> nanofluid is found higher when compared to others and the same is indicated in fig. 10.

### Effect of pipe inclination

The thermal efficiency of thermosyphon is calculated by ratio of cooling capacity rate of condenser and the input power at the evaporator section. Figure 11 shows the thermal efficiency difference of thermosyphon based on the variation in tilt angles and it is noted that thermal performance increases with the increase in the angle of inclination. It is due to increase in temperature of working medium and hence there is a possibility of more amount of heat being removed in the condenser section. Here, gravitational force also a cause on the flow of working fluid from the evaporator section to the condenser section.

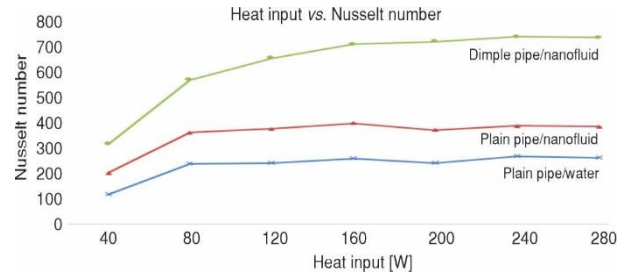


Figure 10. Nusselt number at 90° inclination thermosyphon

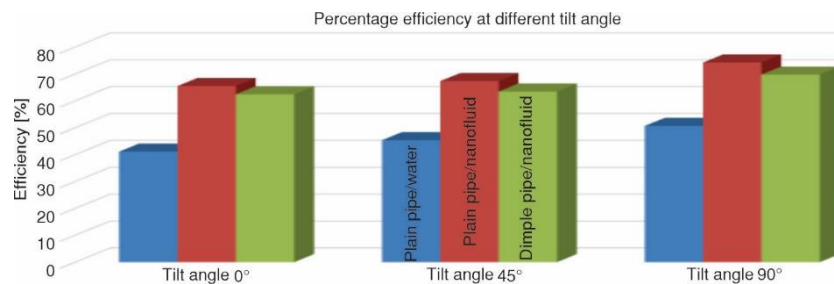


Figure 11. Efficiency at different angle

But at 90°, the efficiency is slightly maximum. Due to increased rate of formation of liquid film inside the condenser, the value of the thermal resistance is increased. So, the heat transfer efficiency of the test thermosyphon increases with nanofluid as compared to that of the base working fluid. Also the dimpled thermosyphon comparatively has obtained higher efficiency than plain thermosyphon.

### Conclusion

This experimental research has reported the performance of thermosyphon and dimpled thermosyphon with water and Al<sub>2</sub>O<sub>3</sub> nanofluid and results have concluded the outcomes below.

For given heat inputs, the estimated efficiency for plain thermosyphon-water is 41.1%, 62.4%, and 65.5%, for plain thermosyphon-Al<sub>2</sub>O<sub>3</sub> nanofluid is 45.36%, 63.41%, and 67.34%, for dimple thermosyphon-nanofluid is 50.66%, 69.7%, and 74.23% at 0°, 45°, and 90°, respectively. Here, the thermosyphon with 90° tilt angle provided the optimal performance as it exhibits maximum efficiency value in all thermosyphons and also dimpled tube thermosyphon exhibits high efficiency than plain pipe.

The thermal resistance for plain thermosyphon-water varies from 0.19 °C/W to 0.55 °C/W, for plain thermosyphon-nanofluid is 0.1 °C/W to 0.39 °C/W, for dimpled thermosyphon-nanofluid is between 0.089 °C/W to 0.34 °C/W. The thermal resistance value is minimum in dimple thermosyphon-nanofluid which implies more heat will be transferred using dimple.

The average heat input required for a cycle is estimated for  $0^\circ$ ,  $45^\circ$ , and  $90^\circ$  as 160.75 W, 160.05 W, and 160.28 W, respectively. This indicates there is no much difference in heat input, but orientation of  $0^\circ$  consumes more than the other two angles of orientation.

With increase in heat input the Nusselt number value is found to be increasing and it is found to be high in dimpled thermosyphon than the plain thermosyphon with nanofluid and water.

The performance of thermosyphon at  $90^\circ$  provides the higher efficiency than other two angles of  $0^\circ$  and  $45^\circ$ . In addition to that thermosyphon with dimpled surface has provided the highest efficiency amongst all the three samples. So, the experimental results are supporting the dimple thermosyphon's performance for heat transfer applications.

## References

- [1] Raju, T., *et al.*, Experimental Investigation of Solar Evacuated Tube Collector with Multi-Walled Carbon Nanotube-Water-Based Nanofluid, *Energy Sources, Part A: Recovery, Utilization, and Environmental Effects*, 45 (2023), 1, pp. 924-939
- [2] Lu, C. Lv., *et al.*, Micro Flat Heat Pipes for Microelectronics Cooling: Review, *Recent Patents on Mechanical Engineering*, 6 (2013), 3, pp. 169-184
- [3] Mohamed, H. A. Elnaggar., *et al.*, The Optimization of Thickness and Permeability of Wick Structure with Different Working Fluids of L-Shape Heat Pipe for Electronic Cooling, *Jordan Journal of Mechanical and Industrial Engineering*, 8 (2014), 3, pp. 119-125
- [4] Su, H., *et al.*, Experimental Investigation on Heat Extraction Using a Two-Phase Closed Thermosyphon for Thermoelectric Power Generation, *Energy Sources, Part A: Recovery, Utilization, and Environmental Effects*, 40 (2018), 12, pp. 1485-1490
- [5] Kumaresan, G., *et al.*, An Experimental Study on Improvement in Thermal Efficiency of Mesh wick Heat Pipe, *Applied Mechanics and Materials*, 592-594 (2014), July, pp. 1423-1427
- [6] Weng, Y. C., *et al.*, Heat Pipe with PCM for Electronic Cooling, *Applied Energy*, 88 (2011), 5, pp. 1825-1833
- [7] Manikanda P. N., *et al.*, Heat Transfer Analysis of Looped Heat Micro Pipes with Graphene Oxide Nanofluids for Li-Ion Battery, *Thermal Science*, 25 (2020), 1A, pp.387-397
- [8] Rao, Z., *et al.*, Experimental Investigation on Thermal Management of Electric Vehicle Battery with Heat Pipe, *Energy Conversion and Management*, 65 (2013), Jan., pp. 92-97
- [9] Tian, M.-W., *et al.*, Economic Cost and Efficiency Analysis of a Lithium-Ion Battery Pack with the Circular and Elliptical Cavities Filled with Phase Change Materials, *Journal of Energy Storage*, 52 (2022), 2, 104794
- [10] Ayompe, L. M., *et al.*, Thermal Performance Analysis of a Solar Water Heating System with Heat Pipe Evacuated Tube Collector Using Data from a Field Trial, *Solar Energy*, 90 (2013), Apr., pp. 17-28
- [11] Dan, N. N., *et al.*, Performance Analysis and Comparison of Concentrated Evacuated Tube Heat Pipe Solar Collectors, *Applied Energy*, 98 (2012), Oct., pp. 22-32
- [12] Ram, R., *et al.*, Analysis of the Wicking and Thin-Film Evaporation Characteristics of Wick Micro-Structures, *ASME Journal of Heat transfer*, 131 (2009), 10, pp. 1-11
- [13] Madhusree, K., *et al.*, Thermal Performance of Screen Mesh Wick Heat Pipes Using Water-Based Copper Nanofluids, *Applied Thermal Engineering*, 50 (2013), 1, pp. 763-770
- [14] Kumaresan, G., *et al.*, Experimental Study on Effect of Wick Structures on Thermal Performance Enhancement of Cylindrical Heat Pipes, *Journal of Thermal Analysis and Calorimetry*, 136 (2019), 1, pp. 389-400
- [15] Zhang, Z., *et al.*, Experimental and Numerical Study of a Passive Thermal Management System Using Flat Heat Pipes for Lithium-Ion Batteries, *Applied Thermal Engineering*, 166 (2019), 114660
- [16] Liu, Z.-Q., *et al.*, Thermal Performance of Inclined Grooved Heat Pipes Using Nanofluids, *International Journal of Thermal Sciences*, 49 (2010), 9, pp. 1680-1687
- [17] Manikanda, N. P., *et al.*, Investigation of Heat Transfer Enhancement Effect on Normal and Nano Coated Wick Structure Heat Pipes-A Comparative Assessment, *International Journal of Engineering Research in Africa*, 51 (2020), Nov., pp. 191-198

- [18] Vijayakumar, M., *et al.*, A Study on Heat Transfer Characteristics of Inclined Copper Sintered Wick Heat Pipe Using Surfactant Free CuO and Al<sub>2</sub>O<sub>3</sub> Nanofluids, *J. Taiwan Inst. Chem. Eng.*, 81 (2017), Dec., pp. 190-198
- [19] Godson, A. L., *et al.*, Heat Transfer Performance of Screen Mesh Wick Heat Pipes Using Silver-Water Nanofluid, *International Journal of Heat Mass Transfer*, 60 (2013), 1, pp. 201-209
- [20] Nallusamy, S., *et al.*, Heat Transfer Enhancement Analysis of Al<sub>2</sub>O<sub>3</sub>-Water Nanofluid through Parallel and Counter Flow in Shell and Tube Heat Exchanger, *International Journal of Nano Science*, 16 (2017), 05-06, 1750020
- [21] Liu, Z. H., *et al.*, Application of Aqueous Nanofluids in a Horizontal Mesh Heat Pipe, *Energy Conversion Management*, 52 (2011), 1, pp. 292-300
- [22] Kumaresan, G., *et al.*, Experimental Investigation on Enhancement in Thermal Characteristics of Sintered Wick Heat Pipe Using CuO Nanofluids, *International Journal of Heat and Mass Transfer*, 72 (2014), May, pp. 507-516